Articles

Mechanism of Unfolding of a Model Helical Peptide†

Belinda Pastrana-Rios*

Departmentof Chemistry, University of Puerto Rico Mayagüez Campus, Mayagüez, Puerto Rico 00681-9019

Received February 26, 2001; Revised Manuscript Received May 30, 2001

ABSTRACT: Synthetic model helical peptides, Acetyl-W(EAAAR)$_5$A-amide with ^{13}C═O specifically labeled alanine segments in repeats $n = 1,2$ or 4,5 were studied in aqueous D_2O solution as a function of temperature using Fourier transform infrared spectroscopy and two-dimensional correlation analysis. The ^{13}C═O provided a probe which was sensitive to the carbonyl stretch in the peptide bonds of the alanine residues at the amino terminal end in one peptide as compared to the probe in the carboxy terminal end of the other peptide during thermal perturbation. The relative stability of each terminal end was examined; the more stable terminal was determined to be the amino terminal end. Also studied were the glutamate and arginine side-chain modes involved in the salt bridging interaction. Two-dimensional correlation analysis enabled enhanced resolution in the spectral region of 1520−1700 cm^{-1}, and thus, the order in which these vibrational modes were perturbed as a function of increasing temperature were established.

Marqusee and Baldwin (*1*) as well as Shoemaker (*2*) first studied peptides of variable chain length and their tendency for helical conformation in aqueous solution. Marqusee's group also studied variably spaced Glu$^-$/Lys$^+$ salt bridges to probe the stabilizing effect this weak interaction had on the helix structure by circular dichroism (CD).[1] This study was extended by Stellwagen's group (*3*−*6*) in early 1990s to further study residue replacement within the alanine sequence repeat in Ac-YEAAAKEAXAKEAAAKA-amide to explore the helix dipole and the salt bridges within this model peptide. They also studied the effects caused by pH and ionic strength on the stability of the helix. A model alpha-helical peptide [Ac-W(EAAAR)$_n$A-NH$_2$], first studied by Stellwagen's group (*7*−*10*) using CD and NMR was also used to study helicity. In the late 1990s Prendergast group (*11*) revisited the chain length dependence study using the following peptide sequence Ac-W(EAAAR)$_n$A-NH$_2$ for $n =$ 1−7 via FT-IR, two-dimensional correlation analysis and CD. This peptide has proven to be insightful in regards to its secondary structure and its stability during thermal unfolding.

Two-dimensional correlation analysis was first described by Noda (*12*−*15*) as a technique that could resolve complex bands such as the amide I band. Since 1989 this technique has been applied to the study of H→D exchange in proteins (*16*, *17*), protein unfolding (*18*, *19*), and in the study of model peptides (*11*). In the present study, correlation analysis was performed as described by Graff (*11*). Briefly, the dynamic spectral information is obtained as $D_{v,t}$ using

$$D_{v,t} = F_{v,i} - A'_v \text{ for } i = 1 \text{ to } t \quad (1)$$

where $F_{v,i}$ is the matrix representation of the experimental data as a function of frequency, v; perturbation, t and A'_v is the average of all spectra measured within the temperature range of interest.

A complex matrix $C_{v,f}$ is generated using the dynamic spectral information. The cross-correlation of this matrix is the cross product of itself with the transpose of its complex conjugate $\overline{C^T_{v,f}}$.

$$C_{v,f} \times \overline{C^T_{v,f}} = \mathrm{Re}[I_{v1,v2}] + \mathrm{Im}[I_{v1,v2}] = \theta_{v1,v2} + \psi_{v1,v2} \quad (2)$$

where $I_{v1,v2}$, is the cross correlation intensity matrix, for the real and imaginary parts which represent the synchronous correlation, $\theta_{v1,v2}$, and asynchronous correlation, $\psi_{v1,v2}$, respectively.

Reported herein are the results of two-dimensional correlation and curve-fit analysis performed on the infrared spectra of two specifically labeled ^{13}C helical peptides as a function of temperature. These labeled peptides were used to probe the stability of the carboxy and amino terminal ends of a model helical peptide, Ac-W(EAAAR)$_5$A-NH$_2$. This approach has allowed for the simultaneously study of ^{12}C and ^{13}C labeled carbonyl stretching modes, as well as the carboxylate vibrations of the glutamate side chains, and hence describe the thermal unfolding mechanism of an α-helical structure.

EXPERIMENTAL SECTION

Materials. The materials were all of the highest purity commercially available and were used without further

† This research was supported by NSF-EPSCoR, the University of Puerto Rico, Mayagüez Campus and the Mayo Clinic Foundation.

* To whom correspondence should be addressed. Phone: (787) 832-4040 ext. 2302. Fax: (787) 265-3849. E-mail: belinda@hpcf.upr.edu.

[1] Abbreviations: FT-IR, Fourier transform-infrared; CD, circular dichroism; 2D-FT-IR, two-dimensional Fourier transform-infrared; D_2O, deuterium oxide; TFA, trifluoroacetic acid; CaF_2, calcium fluoride; TOF, time-of-flight mass spectrometry.

10.1021/bi0155145 CCC: $20.00
Published on Web 07/11/2001

purification. Deionized H_2O (18 MΩ) and D_2O 99.9% Atom D (Cambridge Isotope Laboratories, Inc., Andover, MA) were used as indicated below. Phosphate buffer, 1 mM (Sigma Chemical Co., St. Louis, MO), 10 mM NaCl in 99.9% D, and D_2O at pD = 6.6 were used for spectroscopic studies. The model helical peptide, ^{13}C-labeled peptide bond carbonyls for alanines in $n = 1,2$ or 4,5 for Ac-W(EAAAR)$_5$-A-NH_2 were synthesized at the protein core facility at Mayo Clinic Foundation. These synthetic peptides were subjected through two steps in preparation of the sample for FT-IR spectroscopic studies. The first was extensive dialysis against 0.1 N HCl to remove trifluoracetic acid (TFA). Second, was the complete H→D exchange by repeated lyophilization and redissolving the sample and reference in D_2O. Trifluoroacetic acid (TFA) from Sigma Chemical Co., in St. Louis, MO was used for spectral subtraction of traces of this compound from the desired sample.

Methods: FT-IR Spectroscopy. To perform the FT-IR experiment fully H→D exchanged peptide the sample was redissolved in 1 mM phosphate buffer, 10 mM NaCl in 99.9% D, D_2O at pD = 6.6. A 25 μL aliquot of 48 mg/mL of the peptide was deposited on a 49 mm × 4 mm custom milled CaF_2 window with a 41 μm path length and a second CaF_2 window was used to seal the sample. A reference cell was prepared similarly. Temperature within the cell was controlled via a Neslab circulating bath (Newington, NH) and monitored with a thermocouple positioned in close contact with the sample. The temperature accuracy was estimated to be within 1 °C. Routinely, 10 min were allowed for thermal equilibrium to be reached before spectral acquisition was begun. The instrument used for these experiments was an FTS-40 Bio-Rad (Cambridge, MA) with custom sample shuttle and interface. Typically, 512 scans were co-added, apodized with a triangular function and Fourier transformed to provide a resolution of 4 cm^{-1}, with data encoded every 2 cm^{-1}. Sixteen spectra were collected at sequential increments of temperature, allowing for thermal equilibrium, and used in the two-dimensional FT-IR correlation analysis. TFA spectra were obtained using a Mattson Infinity series 60 MHz interferometer with a shuttle and custom built dual chamber cell holder. The instrument was continuously purged with a dry air generator from Whatman. This TFA sample was applied between two 49 mm × 4 mm custom milled CaF_2 windows (Spectral Systems, Hopewell Junction, NJ) with a 40 μm path length in a similar manner as described above. Spectral data for the TFA sample was obtained by acquiring 512 scans and apodized with a triangular function and Fourier transformed to provide a resolution of 4 cm^{-1} with data encoded every 2 cm^{-1}.

Two-dimensional FT-IR correlation analysis was performed using MathCad 2000 Professional (MathSoft, Inc., Cambridge, MA) software. The curve-fitting routines were done using Grams 3.01 (Galactic Industries Corp., Salem, NH) program. Origin 6 program was used to plot curve-fitted data.

RESULTS

FT-IR Spectroscopy. Typical FT-IR spectra at $T = 20$ °C, for the fully exchanged H→D labeled ($n = 1,2$ and $n = 4,5$) peptides, in the spectral region of 1300−1750 cm^{-1} are shown in Figure 1. The band assignments for the spectral region of 1520−1750 cm^{-1} are comprised of the overlapped bands at 1635 cm^{-1} for the amide I′ band (*20*−*24*) at 1598 cm^{-1}, the amide I*′ band (labeled and H→D exchanged) (*25*−*27*), at 1550 cm^{-1} (glutamate) and 1585 and 1611 cm^{-1} are the arginine symmetric and asymmetric stretch, respectively. Furthermore, in the spectral region of 1400−1300 cm^{-1}, at 1450 cm^{-1} are the HOD bending and N−D deformation bands which overlap each other and several lower intensity bands to be assigned in a future study. These bands include the CH_2 scissoring, end methyl, the amide III band and several carboxylate vibrational modes. The intensity of the HOD band as compared to the amide I′ band is indicative of a fully exchanged peptide thus allowing for subsequent study of the side-chain modes involved in salt bridging interaction within this peptide. These side-chain modes have been assigned previously by Chirdgadze (*28*). Superimposed spectra at 20 °C of the unlabeled peptide and the $n = 1,2$ labeled peptide are shown in Figure 2. The additional shoulder at 1598 cm^{-1} observed only in the labeled peptide spectrum, is assigned as that of the ^{13}C═O labeled α-helix band. Thus, shifting the α-helix band by about 37 cm^{-1}, from 1635 cm^{-1} (unlabeled α-helix) to 1598 cm^{-1} (labeled α-helix). The labeled peptides were subjected to thermal perturbation and typical spectra are shown in Figure 3. The overlaid spectra shown in Figure 3, have been TFA subtracted and baseline corrected, no other data manipulation

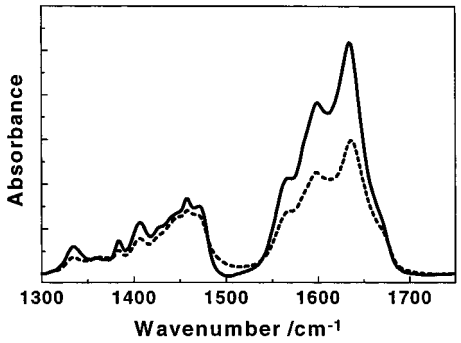

FIGURE 1: Overlaid spectra of fully H·D exchanged ^{13}C═O labeled peptides [Ac-W(EAAAR)$_5$A-NH_2] in the spectral region of 1300−1750 cm^{-1}, at 20 °C in 10 mM phosphate buffer at pD 6.6; (—) alanine labeled carbonyls in $n = 4,5$ repeats and (- - -) $n = 1,2$ alanine segment labeled carbonyls. The spectral features shown are the overlapped amide I′ and amide I*′ bands, glutamate and arginine side-chain modes, and overlapped HOD and N−D deformation bands.

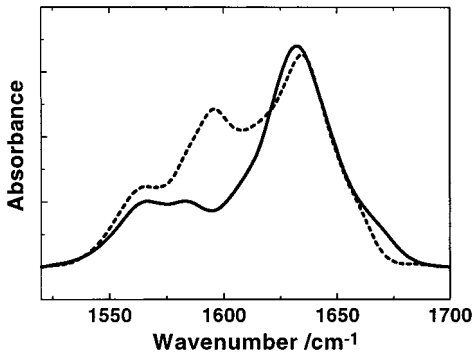

FIGURE 2: Superimposed spectra of Ac-W(EAAAR)$_5$A-NH_2 (—) [from previously published work (11)] and the $n = 1,2$ ^{13}C═O labeled Ac-W(EAAAR)$_5$A-NH_2 (- - -) in the spectral region of 1520−1700 cm^{-1} at 20 °C. The spectra have been normalized and baseline corrected.

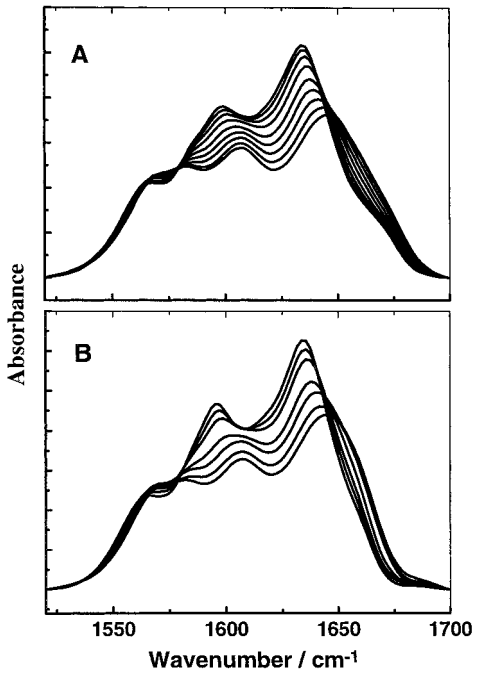

FIGURE 3: Overlaid spectra of ^{13}C labeled peptides in the spectral region of 1520−1700 cm^{-1} from −2 to 85 °C (A) $n = 4,5$ and (B) $n = 1,2$. The spectra have only been baseline corrected and residual TFA subtracted.

was performed. Subtraction of this narrow band was done mainly to simplify the 2D-FT-IR plots. Spectral features shown in Figure 3 are due to the sum effect of the labeled and unlabeled backbone, as well as the side-chain vibrational modes, yet characteristic band shifts due to thermal unfolding can still be discerned. Changes in the spectral features such as intensity and position are observed for the amide I′, amide I*′ bands and side chains suggesting that all modes are thermally affected and that denaturation of the peptide has occurred.

2D-FT-IR. The use of 2D-FT-IR to resolve complex bands has been proven to be useful in this study as shown in Figures 4 and 5. In general, a position specific thermal denaturation study was carried-out by monitoring the auto peaks and cross-peaks associated with the α-helical bands (labeled and unlabeled). For the 2D-plots, the spectral data acquired was divided into two data sets as pre-thermal transition (temperature interval 0−40 °C) and the post-thermal transition (temperature interval 40−85 °C). As a result, eight spectra were analyzed in each two-dimensional correlation analysis shown in Figures 4 and 5. The average of each data set was used to obtain the dynamic spectral information. However, the first temperature spectrum, for each data set, was also used to obtain the dynamic spectral information (*data not shown*) and no appreciable differences on the synchronous and asynchronous contour plots were observed; only the intensity of the peaks was affected. For reasons of direct comparison with previously published work, the results reported herein include only the average spectral comparison.

Synchronous 2D-IR Correlation Analysis. Information on the vibrational modes that are changing due to the perturbation can be discerned directly from the auto peaks observed in the synchronous plots. The assignment of the auto peaks for the synchronous contour plots in Figures 4 and 5, comprise of 1550 cm^{-1} (glutamate), 1599 cm^{-1} ($^{13}C{=}O$ labeled α-helix), 1630 cm^{-1} (unlabeled α-helix), and at 1660 cm^{-1} (random coil). The auto peak at 1599 cm^{-1} due to the $n = 4,5$ $^{13}C{=}O$ labeled α-helix has the characteristic ridges as described previously (*11*), this auto peak loses the ridge appearance at high temperature and is shifted by about 3 wavenumbers to 1601 cm^{-1} (Figure 4C), suggesting that the thermal denaturation process has already occurred at the carboxy terminal end of the peptide. The $n = 1,2$ labeled α-helix band is also shifted upon increasing temperature from 1598 cm^{-1} (Figure 5A) to 1600 cm^{-1} (Figure 5C). Contrary to the $n = 4,5$ labeled peptide, the $n = 1,2$ labeled peptide is still undergoing thermal transition at high temperatures, thus suggesting that the amino terminal end undergoes unfolding after the carboxy terminal end. Furthermore, in Figure 4, panels A and C, and Figure 5, panels A and C, are the auto peaks for the unlabeled α-helix band at 1636 cm^{-1} with its characteristic ridges, due to the shifting of this band (1620−1651 cm^{-1}) in response to the thermal denaturation process. The random coil observed at 1660 cm^{-1} (Figures 4A and 5A) and 1670 cm^{-1} (Figures 4C and 5C), which result from the unwinding of the helix. The glutamate auto peak at 1550 cm^{-1} for the $n = 4,5$ labeled peptide is not observed in the synchronous plot that comprise spectra above the transition temperature (40−80 °C) of the peptide shown in Figure 4C. This result is consistent with the asynchronous plot discussed below. The absence of this peak in the plot at high temperature is due to the lack of change in frequency and intensity of this band in this temperature interval. Yet, this glutamate peak is still present in the $n = 1,2$ labeled peptide at high-temperature Figure 5C. Thus, confirming that the carboxy terminal end undergoes unfolding prior to the amino terminal end. More importantly, is the presence of the 1575 cm^{-1} peak due to the arginine symmetric stretch, which is shown in Figure 5A, but is absent above the transition temperature Figure 5C. The disappearance of this 1575 cm^{-1} peak (arginine symmetric stretching mode) is due to the breaking of the salt bridge interaction. In addition, this concomitant shift of the glutamate side-chain band with that of the α-helix suggest that the helix is stabilized by both the hydrogen bonding and the salt bridging between the side-chain carboxylates and the primary amines of the arginine residues. More importantly, the salt bridge interaction could also explain the unusually low wavenumber observed for the α-helix band at 1630 cm^{-1}. The vibrational mode of the peptide carbonyls is affected by the rigidity of the helix. As shown for this model peptide, the flexibility of this helix is limited by the salt bridging that is formed between the glutamate and the arginine. Similar results have been reported by others (*1*, *6*−*8*).

The sign of the cross-peaks in these synchronous plots can be associated with frequency changes that occur simultaneously as proposed by Noda (*13*−*15*). These changes in frequency occur because the dipole moment of different functional groups are reorienting simultaneously and are strongly interacting. This event would define a cooperative effect. Positive cross-peaks indicate that the reorientation is similar while, the negative cross-peaks indicate different reorientations of the functional groups involved. The synchronous plots shown in Figures 4 and 5, have positive cross-peaks associated with the labeled and unlabeled helix (1600 and 1636 cm^{-1}, respectively) and glutamate band (1565 cm^{-1}), suggesting same reorientation of the dipole moment.

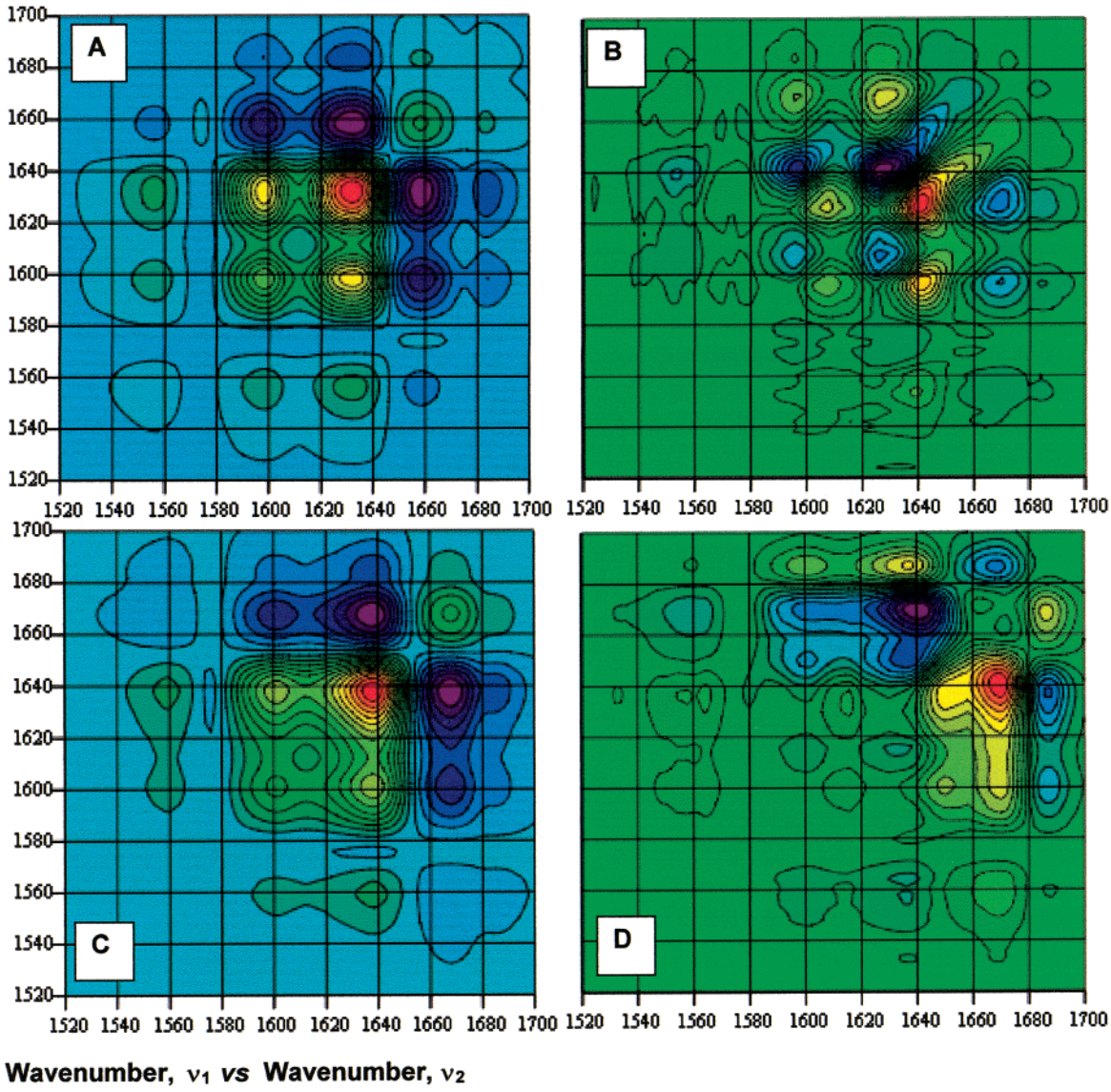

FIGURE 4: Two-dimensional correlation plots for the $n = 4,5$ $^{13}C{=}O$ labeled peptide below the transition temperature (i.e., 0−40 °C). (A) Synchronous and (B) asynchronous, and above the transition temperature (i.e., 40−85 °C). (C) Synchronous and (D) asynchronous.

Meanwhile, the random coil band (1660 cm^{-1} shown in Figures 4A and 5A or 1670 cm^{-1} shown in Figures 4C and 5C) has associated cross-peaks that are negative, therefore having a different reorientation than that observed for the α-helix and glutamates.

Although the synchronous plot has not been used to determine the chronological order of events, in this study it is possible to highlight several of these events due to the separation of the spectral data into two separate temperature intervals (pre- and post-thermal transition). The glutamate auto peak is non existent (no change due to perturbation is occurring) at high temperatures (Figure 4C), suggesting the salt bridge interaction has been broken in the $n = 4,5$ labeled peptide. This event is followed by the disappearance of the ridge effect in the labeled α-helical band suggesting the carboxy terminal end has undergone transition. The unfolding of the carboxy terminal end is followed by breaking of the glutamate/arginine salt bridge a band at 1575 cm^{-1} (Figure 5A) associated exclusively with the side-chain modes as determined from simulation studies performed (*manuscript in preparation*). The breaking of the salt bridges at the carboxy terminal end is followed by the transition of the labeled α-helical band (Figure 5C). The glutamate band is still present in the synchronous plot at high temperatures, suggesting that the glutamate side chain at the amino terminal end is still being thermally perturbed. Finally, the labeled α-helical band is observed to have the ridge effect also suggesting continued thermal transition, at the amino terminal end.

Asynchronous 2D-IR Correlation Analysis. The asynchronous plots shown in panels B and D in Figures 4 and 5, provide information on the decoupling events that occur for the $n = 4,5$ and $n = 1,2$ peptide, respectively. Several cross-peaks, shown in Figure 4B, associated with the arginine modes (symmetric and asymmetric stretch) at 1600−1575 cm^{-1} suggest that these vibrational modes are not coupled. In addition, the 1600−1630 cm^{-1} (arginine asymmetric stretch and the unlabeled α-helix band) are also none interacting. These cross-peaks are absent in the asynchronous plot after the thermal transition has occurred (Figure 4D), thus suggesting that these arginine peaks are no longer changing. These results were confirmed in the simulation carried out (data not shown). Similarly, the asynchronous plots for the $n = 1,2$ peptide (Figure 5, panels B and D).

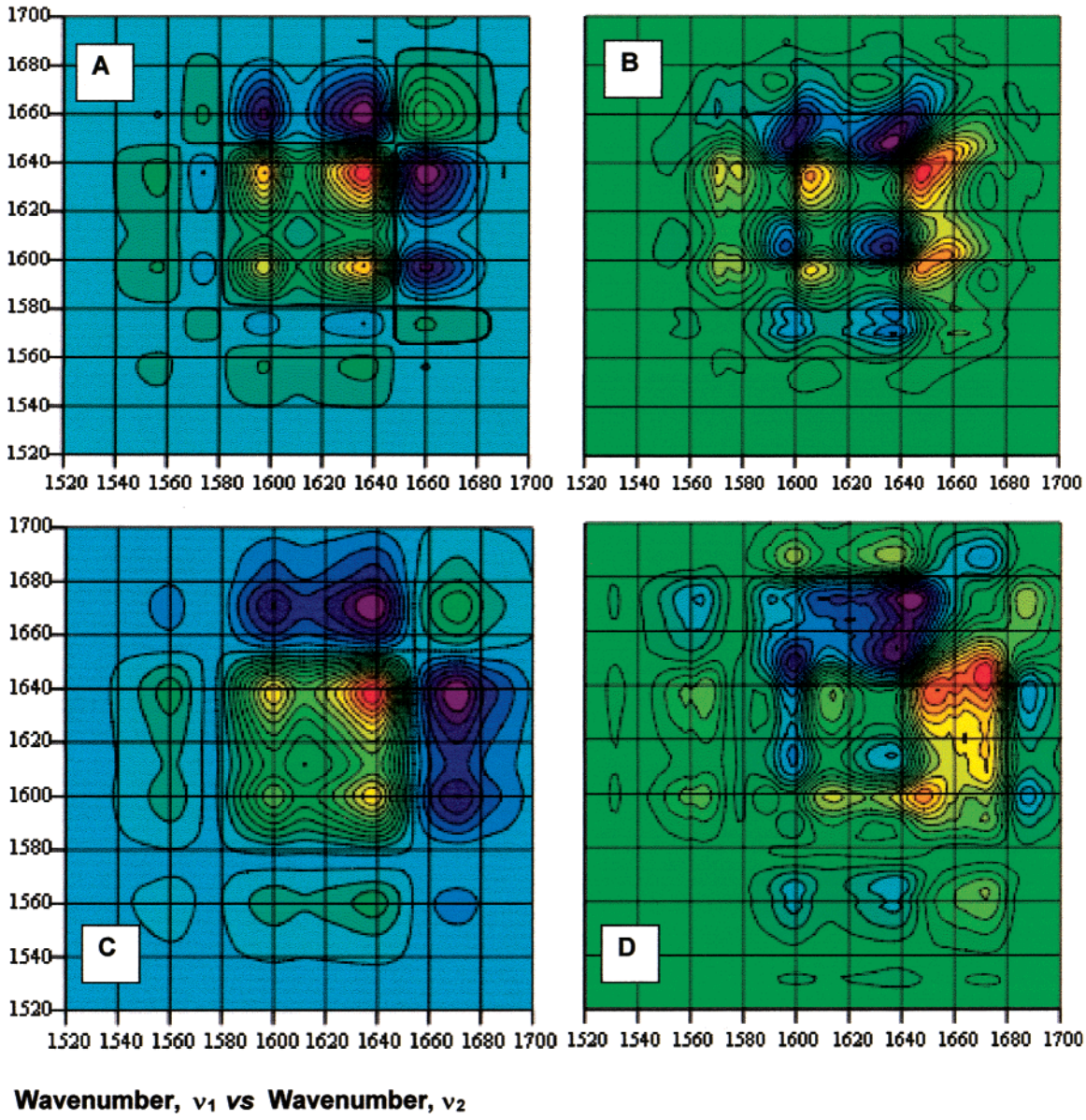

FIGURE 5: Two-dimensional correlation for the $n = 1,2$ $^{13}C{=}O$ labeled peptide below the transition temperature (i.e., 0−40 °C). (A) Synchronous and (B) asynchronous, and above the transition temperature (i.e., 40−85 °C). (C) Synchronous and (D) asynchronous plots.

The cross-peaks at 1558−1570 cm^{-1} (glutamate and arginine symmetric stretch, respectively) are present at low temperature (Figure 5B), but absent at the temperature interval 40−85 °C (Figure 5D), suggesting that there is a change in the nature of the interaction.

Once the nature of the interaction has been established during the thermal unfolding process, then one can determine the order of events for this model peptide. The $n = 4,5$ labeled peptide shown in Figure 4, panels B and D, can be summarized as the break of salt bridge interaction (1575 cm^{-1}, arginine symmetric modes are no longer present), followed by the random coil (1670 cm^{-1}) changing prior to the labeled helix (1611 cm^{-1}) which in turn undergoes transition prior to the unlabeled helix (1640 cm^{-1}). Furthermore, for the $n = 1,2$ labeled peptide shown in Figure 5, panels B and D, can be summarized as follows. The glutamate (1550 cm^{-1}) and arginine (1575 cm^{-1}) salt bridge interaction breaks followed by the random coil (1670 cm^{-1}) changes prior to the unlabeled helix (1640 cm^{-1}) and as a last transition, is the labeled helix at 1611 cm^{-1}. These results agree with the results described in the synchronous plots described above.

Curve-Fitting Analysis. The number of bands and their positions were determined from the two-dimensional plots shown in Figures 4 and 5. The author is assuming two things. First, that the random coil band for the $^{13}C{=}O$ labeled portion of the peptide is very low in intensity and will not be considered for this curve-fitting analysis. Second, the overall effect observed in the unlabeled random coil band will be the same as that of the $^{13}C{=}O$ labeled random coil mode. Typical, curve-fitted spectra are shown in Figures 6 and 7. All of the subbands used in the fit have been properly assigned to a particular vibration and were corroborated by the band positions determined in the 2D-FT-IR plots according to the temperature range the spectrum was acquired. In addition, simulation of the 2D-FT-IR plots (*manuscript in preparation*) for the amide I′* band along with the glutamate vibration for spectra obtained above the peptides transition temperature rendered similar contour features, thus increasing the confidence in the procedure used for this study.

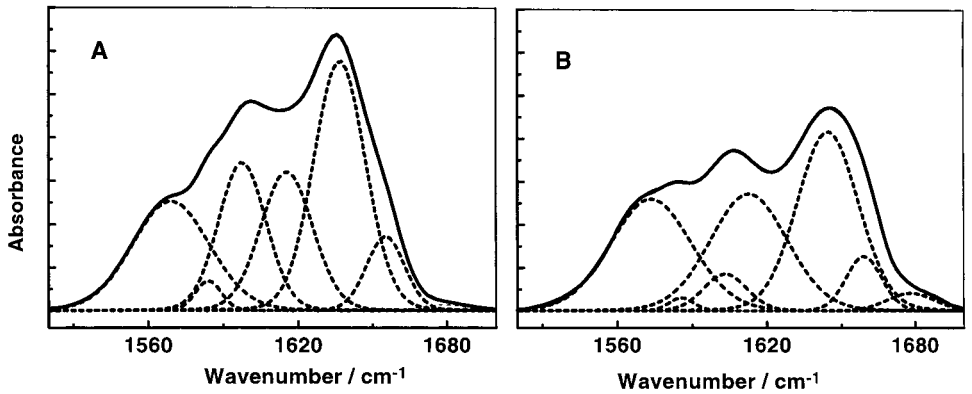

FIGURE 6: Typical curve-fitted spectra of $^{13}C{=}O$ labeled peptide at the $n = 4,5$ end at (A) 20 °C and (B) 80 °C. All subbands used for the curve-fit have been assigned to a vibrational mode.

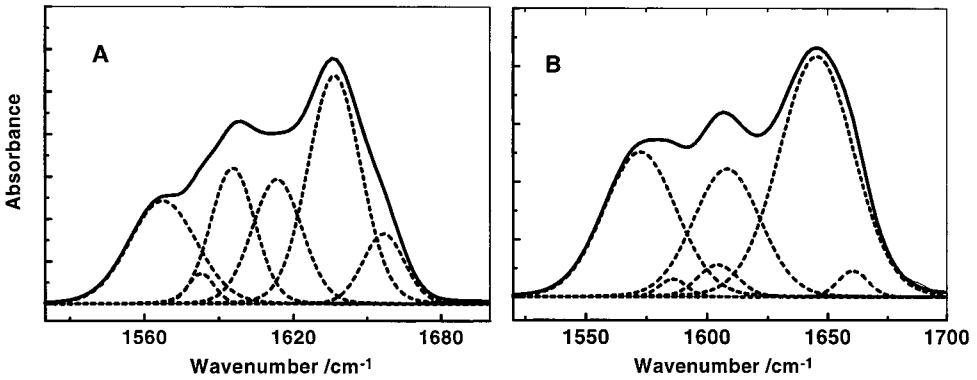

FIGURE 7: Typical curve-fitted spectra of $^{13}C{=}O$ labeled peptide at the $n = 1,2$ end at (A) 20 °C and (B) 80 °C. All subbands used for the curve-fit have been assigned to a vibrational mode.

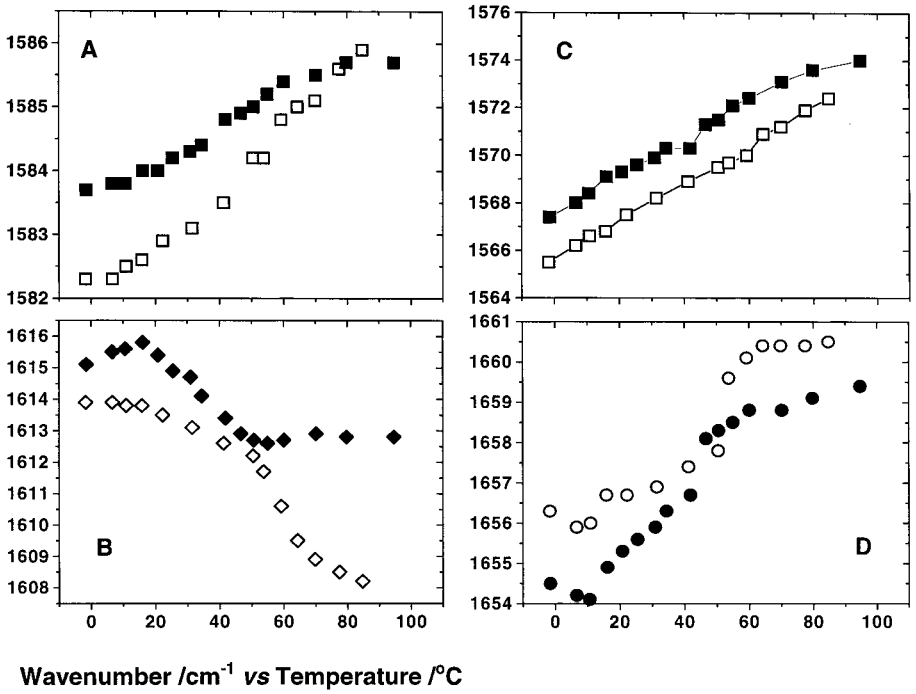

FIGURE 8: Temperature dependence plots for both labeled peptides. In general, the closed symbols are for the $n = 4,5$ labeled peptide and the open symbols are for the $n = 1,2$ labeled peptide: (a) arginine symmetric stretching mode (squares); (b) arginine asymmetric stretching mode (diamonds); (c) glutamate stretching mode (connected squares); (d) random coil band (circles).

Frequencies for each subband were plotted as a function of temperature are shown in Figures 8 and 9. These results are in good agreement with those reported for the chain length dependence study (*11*) and also corroborate the cooperativity suggested in the synchronous plots for these vibrational modes.

In all the temperature dependence plots shown in Figure 8 for the side-chain vibrational modes and the random coil

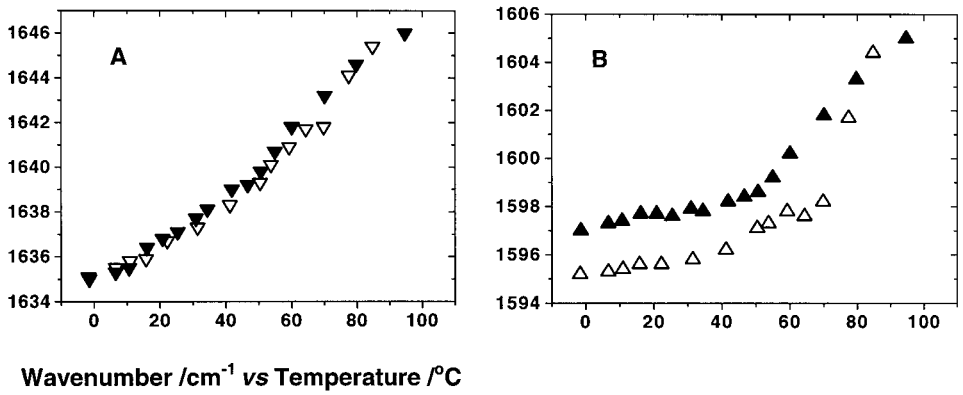

FIGURE 9: Temperature dependence plots of the peptide carbonyl stretching mode for both peptides: (a) unlabeled α-helix (▽) $n = 1,2$ and (▼) $n = 4,5$; (b) labeled α-helix (△) $n = 1,2$ and (▲) $n = 4,5$. A sigmoidal curve is observed suggesting a cooperative thermal transition for both peptides.

band for the $n = 4,5$ labeled peptide, a lower transition temperature is observed, suggesting that the peptide begins to unfold in the $n = 4,5$ end. The arginine symmetric stretch temperature dependence shown in Figure 8A has a different behavior to the arginine asymmetric stretch temperature dependence shown in Figure 8B. The differences in the arginine symmetric and asymmetric curves (Figure 8, panels A and B, respectively) could be due to the coupling of the arginine and the glutamate carboxylates. In addition, the glutamate has a linear dependence with temperature (Figure 8C), this behavior was also observed in the previous work (*11*) suggesting a simple transition (as salt bridge interacting and non-interacting) different from that observed for the arginine side-chain vibrational modes. In Figure 8D, for the random coil subband shows that the thermal transition for the $n = 4,5$ occurs prior to the $n = 1,2$ although the $n = 4,5$ is more stable at low and high temperatures. The temperature dependence plots for the side-chain modes and random coil are in good accord with the temperature dependence plots shown in Figure 9, panels A and B, for the $^{13}C{=}O$ labeled α-helix and the unlabeled α-helix for both peptides. A sigmoidal curve is observed in both plots suggesting a cooperative thermal denaturation process for both peptides. Once again the $n = 1,2$ labeled peptide (Figure 9B) has a higher transition temperature than the $n = 4,5$.

DISCUSSION

The α-helix as a structural motif is very common among proteins, by studying this model helical peptide one can gain insight in the stability of the α-helix and thus carry this information over to proteins with secondary structure motifs comprised of helices. These experiments have also demonstrated the usefulness of 2D-FT-IR to simultaneously study amide I′ and amide I′* bands ($^{13}C{=}O$ labeled peptide carbonyls of certain alanine residues) along with contributing side-chain modes for peptide unfolding. Different regions of the α-helical peptide have been simultaneously studied by using $^{13}C{=}O$ during its synthesis and thus providing position specific information that would enable the investigator to elucidate the mechanism of unfolding. In this study, the amino and carboxy terminal ends were labeled, because the peptide synthesized [Ac-W(EAAAR)$_n$A-NH$_2$] was $n = 5$. Thus, allowing us to probe the peptide during thermal denaturation. Future experiments, to be carried-out in Dr. Frank Prendergast's laboratory at Mayo Clinic, will involve the $n = 6$ peptide with specific $^{13}C{=}O$ label in the terminal ends as well as the middle portion of the peptide.

In this study, TFA was not an issue since the synthetic peptides were extensively dialyzed against 0.1 N HCl and the traces of the contaminant were subtracted from the raw spectra obtained. In addition, the spectra plotted were above and below the peptide's transition temperature, thus enhancing the resolution of the spectra obtained even further. This simplified the resulting two-dimensional plots shown herein. This procedure also achieved a confidence in the temporal assignment of band position observed during the thermal denaturation process.

Future studies will involve the proper band assignment in the spectral region of 1300−1400 cm^{-1} to confirm the carboxylate modes for glutamate and the coupling effects with the methylene vibrational modes of the arginine residue.

Two-dimensional correlation analysis has been used to elucidate this mechanism of peptide unfolding. The phase information obtained suggests that the salt bridge between the glutamates (1567 cm^{-1}) and the arginines (1606 and 1596 cm^{-1}) break prior to the helix unwinding (1599 cm^{-1}, ^{13}C labeled α-helix band) to generate the denatured peptide. In addition, the glutamate cross-peak was correlated to the auto peaks of the unlabeled α-helix and random coil, suggesting a strong interaction and thus defining the cooperativity during thermal denaturation process, i e., one event must occur prior to the other in the order described above with a strong interaction between these vibrational modes.

In the curve-fitting analysis, there is a concomitant decrease in intensity the α-helix subband (1636 cm^{-1}) and increase in intensity the random coil subband (1656 cm^{-1}). In addition, a shift in the glutamate band was also observed, suggesting that this vibrational mode is correlated to the peptides secondary structure. The wavenumber vs temperature plots show a transition temperature of about 60, 75, and 60 °C for the $^{12}C{=}O$ peptide bonds and $^{13}C{=}O$ $n = 1,2$ and $n = 4,5$ peptide bonds, respectively. Thus, suggesting that amino terminal end is more stable than the carboxy terminal end.

The side-chain modes are sensitive to the different dipole transition moments during the thermal unfolding process of the helix. The two-dimensional plots also confirmed the correlation between the side chains and the backbone. The strong correlation between the glutamate cross-peaks and the α-helical and random coil auto peaks suggest that the

glutamate and arginine salt bridge contributes significantly toward the stability of this model peptide.

The unfolding of a helix is actually a sequential change of interactions that were originally present in the helix (i.e., orientation of functional groups, such as the carbonyls in the peptide bonds, are stabilized by intramolecular hydrogen bonding and salt bridging interactions). These experiments demonstrate the usefulness of two-dimensional correlation analysis first described by Noda (*12*−*15*) to provide detailed information on peptide unfolding. Moreover, this method can also be applied to proteins to probe structural changes due to perturbation or due to interactions with other proteins. The use of site-directed isotope labeling can be applied to specific regions of interest in a protein and thus probe the changes that occur. More importantly, determine how these changes affect the proteins structure, stability and function.

ACKNOWLEDGMENT

The author sincerely thanks Dr. Frank Prendergast for the generous supply of the ^{13}C labeled peptide. She also thanks Dr. Dave Braddock for his help in the design of the thermostated cell holder and shuttle. The author would also thank Dr. McCormick's group in the synthesis and TOF-MS for the specifically labeled Ac-W(EAAAR)$_5$A-NH$_2$. The work was supported in part by NSF-EPSCoR, and B.P.R. also gratefully acknowledges the support of training grant HDO7108.

REFERENCES

1. Marqusee, S., and Baldwin, R. L. (1987) *Proc. Natl. Acad. Sci. U.S.A. 84*, 8898−8902.
2. Shoemaker, K. R., Kim, P. S., York, E. J., Stewart, J. M., and Baldwin, R. L. (1987) *Nature (London) 326*, 563−567.
3. Merutka, G., and Stellwagen, E. (1989) *Biochemistry 28*, 352−357.
4. Merutka, G., Lipton, W., Park, S.-H., and Stellwagen, E. (1990) *Biochemistry 29*, 7511−7515.
5. Merutka, G., and Stellwagen, E. (1990) *Biochemistry 29*, 894−898.
6. Park, S. H., Shalongo, W., and Stellwagen, E. (1993) *Biochemistry 32*, 12901−12905.
7. Merutka, G., Dimitrios, M., Bruschweiler, R., and Stellwagen, E. (1993) *Biochemistry 32*, 13089−13097.
8. Shalongo, W., and Stellwagen, E. (1995) *Protein Sci. 4*, 1161−1166.
9. Shalongo, W., Dugad, L., and Stellwagen, E. (1994) *J. Am. Chem. Soc. 116*, 2500−2508.
10. Stellwagen, E., and Shalongo, W. (1998) *Biopolymers 43*, 413−418.
11. Graff, D. K., Pastrana-Rios, B., Venyaminov, S. Y., and Prendergast, F. G. (1997) *J. Am. Chem. Soc. 119*, 11282−11294.
12. Noda, I. (1989) *J. Am. Chem, Soc. 111*, 8116−8118.
13. Noda, I. (1990) *Appl. Spectrosc. 44*, 550−561.
14. Noda, I., Dowrey, A. E., and Marcott, C. (1993) *Appl. Spectrosc. 47*, 1317−1323.
15. Noda, I., Dowrey, A. E., Marcott, C., Ozaki, Y., and Story, G. M. (2000) *Appl. Spectrosc. 54*, 236A−248A.
16. Nabet, A., and Pezolet, M. (1997) *Appl. Spectrosc. 51*, 466−469.
17. Dzwolak, W., Kato, M., Shimizu, A., and Yoshihiro, T. (2000) *Appl. Spectrosc. 54*, 963−967.
18. Shultz, P. C., Barzu, O., and Mantsh, H. H. (2000) *Appl. Spectrosc. 54*, 931−938.
19. Fabian, H., Mantsch, H. H., and Schultz, C. P. (1999) *Proc. Natl. Acad. Sci. 96*, 13153−13158.
20. Bai, Y., Milne, S. J., Mayne, L., and Englander, W. S. (1994) *Proteins 20*, 4−14.
21. Krimm, S., and Bandekar, J. (1986) Vibrational Spectroscopy and Conformation of peptides, polypeptides and proteins. In *Advances in Protein Chemistry* (Anfinsen, C. B., Edsall, T. J., and Richards M. F., Eds.) Vol. 38, pp 181−365, Academic Press, New York.
22. Arrondo, J. L. R., Young, N. M., and Mantsch, H. H. (1988) *Biochim. Biophys. Acta 952*, 261−268.
23. Bandekar, J. (1992) *Biochim. Biophys. Acta 1120*, 123−143.
24. Gillie, K. J., Hochlowski, J., and Arbuckle-Keil, G. A. (2000) *Anal. Chem. 72*, 71R−79R.
25. Hubner, W., Mantsch, H. H., and Casal, H. L. (1990) *Appl. Spectrosc. 44*, 732−734.
26. Tadesse, L., Nazarbaghi, R., and Walter, L. (1991) *J. Am. Chem. Soc. 113*, 7036−7037.
27. Harris, P. I., Robillard, G. T., van Dijk, A. A., and Chapman, D. (1992) *Biochemistry 31* 6279−6284.
28. Chirdgaze, Yu. N., Fedorov, O. V., and Trushina, N. P. (1975) *Biopolymers 14*, 679−695.

BI0155145